Available online at www.sciencedirect.com
ScienceDirect
Journal of Power Sources 173 (2007) 621–625
JOURNAL OF POWER SOURCES
www.elsevier.com/locate/jpowsour

Short communication

Structures and electrochemical performances of pyrolized carbons from graphite oxides for electric double-layer capacitor

Ick-Jun Kim [a,*], Sunhye Yang [a], Min-Je Jeon [a], Seong-In Moon [a], Hyun-Soo Kim [a], Yoon-Pyo Lee [b], Kye-Hyeok An [b], Young-Hee Lee [b]

[a] *Korea Electrotechnology Research Institute, 28-1, Seongju-Dong, Changwon 641-600, Republic of Korea*
[b] *Sungkyunkwan University, Suwon 440-746, Republic of Korea*

Received 24 April 2007; received in revised form 11 June 2007; accepted 16 July 2007
Available online 3 August 2007

Abstract

The structural features and the electrochemical performances of pyrolized needle cokes from oxidized cokes are examined and compared with those of KOH-activated needle coke. The structure of needle coke is changed to a single phase of graphite oxide after oxidation treatment with an acidic solution having an $NaClO_3$/needle coke composition ratio of above 7.5, and the inter-layer distance of the oxidized needle coke is expanded to 6.9 Å with increasing oxygen content. After heating at 200 °C, the oxidized needle coke is reduced to a graphite structure with an inter-layer distance of 3.6 Å. By contrast, a change in the inter-layer distance in KOH-activated needle coke is not observed.

An intercalation of pyrolized needle coke, observed on first charge, occurs at 1.0 V. This value is lower than that of KOH-activation needle coke. A capacitor using pyrolized needle coke exhibits a lower internal resistance of 0.57 Ω in 1 kHz, and a larger capacitance per weight and volume of 30.3 F g^{-1} and 26.9 F ml^{-1}, in the two-electrode system over the potential range 0–2.5 V compared with those of a capacitor using KOH-activation of needle coke. This better electrochemical performance is attributed to a distorted graphene layer structure derived from the process of the inter-layer expansion and shrinkage.

Keywords: Electric double-layer capacitor; Activation procedure; Graphite oxide; Pyrolized carbon; Specific capacitance; Needle coke

1. Introduction

Electric double-layer capacitors (EDLCs) have been widely used as energy storage devices for memory back-up systems, and are receiving considerable attention as a promising high-power energy source for electric devices and hybrid electric vehicles [1–3]. The energy storage mechanism of EDLCs is based on the fact that an electric double-layer is formed at the boundary between the electrode and an electrolyte. In electronic devices requiring higher energy density due to their smaller size, the higher specific volume capacitances of EDLCs is an important factor. However, conventional physically/chemically activated carbons possess a micro-porous structure with a moderately high specific surface area, which has limited the specific volume capacitance to less than 20 F ml^{-1}, due to low electrode density, in two-electrode systems [4].

In recent years, an alkali-activation procedure has been investigated to obtain larger specific volume capacitance from graphitizable carbons. These carbons, activated with alkaline solutions such as KOH, NaOH, and K_2CO_3 at 700–900 °C, exhibit larger specific volume capacitances of 20–30 F ml^{-1} [5–7]. It is reported that the first cycle, that is, electric field activation, makes the electrolyte ions intercalate into the graphene layers of the carbons, which introduces the small pore structure of the electrode. Such structural changes during the first cycle are irreversible and provide larger specific volume capacitance. However, it has been also reported that this process has several problems, such as a high activation cost, corrosion of the activation vessel and the rapid degradation of capacitance during charge–discharge cycling. This electrochemical

* Corresponding author. Tel.: +82 55 280 1668; fax: +82 55 280 1590.
E-mail address: ijkim@keri.re.kr (I.-J. Kim).

0378-7753/$ – see front matter © 2007 Elsevier B.V. All rights reserved.
doi:10.1016/j.jpowsour.2007.07.042

performance may be associated with a high diffusion resistivity of the electrolyte ions to penetrate the graphene units.

In general, the activated carbons that have been developed up to now have a pore structure that is generated by partial etching in the interior of the carbon material. They have different electrochemical characteristics, according to the microstructure of the pores that is adjusted by diverse methods.

As an activation procedure, in this study, the oxidation of graphitizable carbon with dilute nitric acid and sodium chlorate ($NaClO_3$), combined with heat treatment, is attempted to achieve an electrochemically stable active material with a large capacitance. The structural features and the electrochemical performances of pyrolized carbons from graphite oxides are examined in terms of the weight ratio of $NaClO_3$ and carbon, together with the heating temperature. A comparison is made with KOH-activated carbon.

2. Experimental

2.1. Oxidation and heat-treatment conditions of needle cokes

Needle coke derived from coal tar pitch and calcinated at 1100 °C was supplied by Nippon Steel Chemical Co. Ltd. For the oxidation of needle coke, needle coke (5 g) and sodium chlorate (in the range 12.5–50 g) were put in 70 wt.% nitric acid (150 ml), and then stirred at room temperature for 24 h. For comparative purposes, activation of the same needle coke was carried out with KOH (KOH/coke = 4/1, w/w) at 700 °C for 2 h under an argon atmosphere. After oxidation or activation, the needle cokes were washed thoroughly with distilled water and heated under vacuum at 100 and 200 °C. The rate of increase in temperature was 3 °C min^{-1}.

2.2. Preparation of electrode and cell capacitor

Needle cokes, pyrolized from oxidized needle cokes by heating at 200 °C were used as active materials for EDLC. The electrodes were composed of pyrolized needle coke, carbon black as an electric conductor and polytetrafluoroethylene emulsion (PTFE) as a binder in a weight ratio of 80:10:10. The components of the electrode were mixed at 2000 rpm in the solvent to make a slurry. A paste, obtained by drying the slurry, was repeatedly roll-pressed for modification of the sheet-type electrode.

Cell capacitors were constructed with an electrolyte impregnated in the separator sandwiched between the electrodes, whose size was 2 cm × 2 cm. These assemblages were housed in Al-laminated film cells. After an organic electrolyte solution of 1.2 M Et_4NBF_4 (tetraethylammonium-tetrafluoroborate) in acetonitrile solution was introduced, the capacitors were sealed, taking out the leads.

2.3. Structural and electrochemical analyses

The structural changes of the needle cokes were measured by X-ray diffraction using Cu Kα radiation. The micrographs of the polished needle cokes were observed with a field emission scanning electron microscope (SEM). Surface area and pore volume of the needle coke were measured according to the BET method by physical adsorption of nitrogen at 77 K, using an automatic absorption system. Crystal structure analysis was undertaken by Raman spectroscopy. The capacitors were charged and discharged at a constant current of 2 mA cm^{-2} between 0 and 2.5 V with a MACCOR (model no. MC-4) test system. The capacitance was calculated from:

$$C = \frac{it}{V} \quad (1)$$

where t is the time period, V is the voltage change, and I is the constant discharge current.

3. Results and discussion

3.1. Structures of needle cokes oxidized with $NaClO_3 + HNO_3$ and activated with KOH

Table 1 shows the preparation conditions and the properties of needle cokes oxidation-treated with dilute nitric acid and sodium chlorate (the N samples), and activated with KOH (sample K1). The values of O/C for the N samples after 100 °C-heating increase with increase in the ratio of $NaClO_3$/needle coke, and lower values of H/C and O/C in a N sample after 200 °C-heating are obtained. However, the H/C and O/C for the K1 sample have far much lower values, and it is assumed that the heating condition has almost no influence on KOH-activation of needle coke. The data in Table 1 show that the N3 sample after 200 °C-heating has a larger surface area and pore volume of 14 m^2 g^{-1} and 0.02 cm^3 g^{-1} compared with the K1 sample after 200 °C-heating.

Table 1
Preparation and properties of needle cokes oxidation-treated with $NaClO_3 + HNO_3$ and activated with KOH

Sample	Chemical	Reaction condition	Reagent/coke	E.A. (after 100 °C-heating)		E.A. (after 200 °C-heating)		Sp (m^2 g^{-1})	Vpore (cm^3 g^{-1})
				H/C	O/C	H/C	O/C		
N1	$NaClO_3 + HNO_3$	24 h at 25 °C	$NaClO_3$/coke = 2.5/1	0.16	0.10				
N2	$NaClO_3 + HNO_3$	24 h at 25 °C	$NaClO_3$/coke = 5.0/1	0.09	0.16				
N3	$NaClO_3 + HNO_3$	24 h at 25 °C	$NaClO_3$/coke = 7.5/1	0.10	0.30	0.04	0.22	14	0.02
N4	$NaClO_3 + HNO_3$	24 h at 25 °C	$NaClO_3$/coke = 10/1	0.11	0.40				
K1	KOH	2 h at 700 °C	KOH/coke = 4/1	0.02	0.2×10^{-3}	0.03	0.3×10^{-3}	4.3	2×10^{-5}

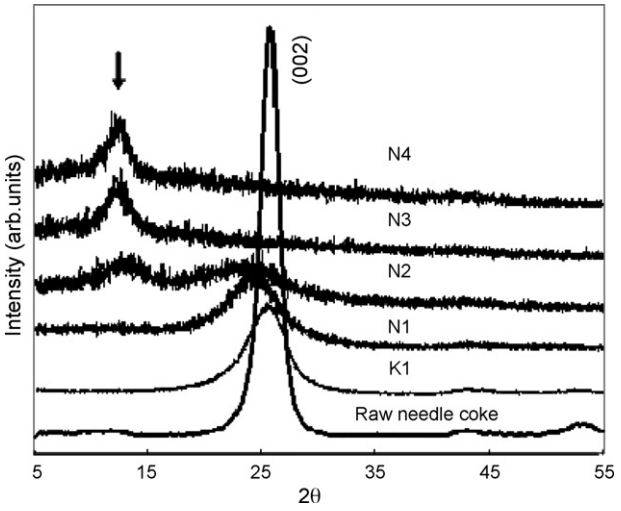

Fig. 1. X-ray diffraction patterns of raw needle coke: N1–N4 after 100 °C-heating and K1 after 100 °C-heating.

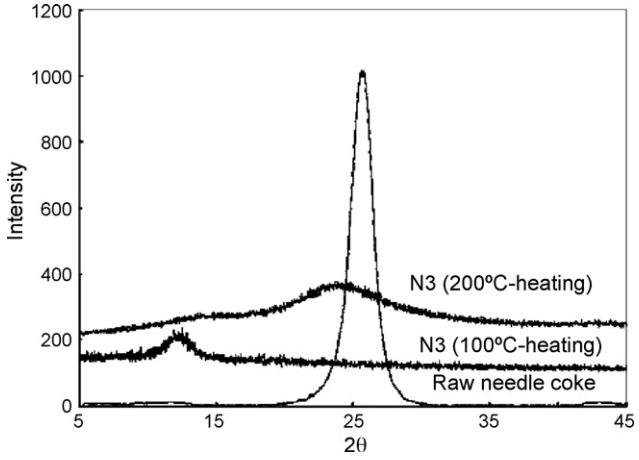

Fig. 3. X-ray diffraction patterns of raw needle coke, N3 after 100 °C-heating, and N3 after 200 °C-heating.

Fig. 1 shows X-ray diffraction patterns of raw needle coke, needle cokes (N1–N4) oxidation-treated and heated at 100 °C, and needle coke (K1) KOH-activated and heated at 100 °C. From a typical graphite structure with (0 0 2) diffraction peak shown in raw needle coke, another diffraction peak at around 12° is observed in needle cokes after oxidation-treatment. This diffraction peak must be attributed to a graphite oxide structure, as reported previously [8,9]. On increasing the composition ratio of $NaClO_3$/needle coke, the diffraction peak of graphite oxide is predominant with the extinction of the graphite structure peak. For the needle cokes oxidation-treated with an acidic solution having an $NaClO_3$/needle coke composition ratio of above 7.5, the single phase of the graphite oxide is observed, and the inter-layer distance of the graphite oxide is calculated to be 6.9 Å. It can be assumed from Fig. 1 that, as the amount of $NaClO_3$ added to the acidic solution increases, the needle coke is more strongly oxidized and the formation of graphite oxide is further facilitated. However, KOH-activated needle coke reduces the intensity and broadens the line width of the (0 0 2) diffraction peak without shifting.

Fig. 2 shows SEM micrographs of the polished plane for (a) raw needle coke, (b) needle coke of N3 after 100 °C-heating, and (c) K1 after 100 °C-heating. From a dense and well-developed layer structure of raw needle coke as shown in Fig. 2(a), the inter-layers of needle coke are expanded after oxidation treatment in Fig. 2(b). This inter-layer expansion is caused by the incorporation of oxygen-containing groups during the oxidation treatment, and proceeds to break down the inter-layer regularity, resulting in broadening of the line width of the graphite oxide peak in the X-ray diffraction pattern. In the case of KOH-activation in Fig. 2(c), partial etching proceeds into the grain by K^+ ions activated at high temperature, and it is difficult to observe expansion between the internal layers.

Fig. 3 shows the X-ray diffraction patterns of raw needle coke, and needle cokes of N3 after 100 and 200 °C-heating. It can be seen that the graphite oxide peak of the N3 sample shifts to 24° ($d_{002} = 3.6$ Å) with a more broadened line width after heating at 200 °C. This reduction in the graphite structure is associated with the thermal decomposition of graphite oxide. As it is well known that thermal decomposition of graphite oxide usually occurs between 150 and 200 °C, heating at 200 °C leads to simultaneous loss of oxygen from each layer plane, resulting in a gradual decrease in layer spacing. In general, thermal decomposition, if the temperature is not increased very slowly, may occur with an almost explosive violence. During heating, the oxygen atoms between the layer planes generally tend to migrate to peripheral surfaces, where they react to form mostly CO or CO_2. The mechanical action of releasing these gases or the carbon depleting from the layer plane may partially fracture the graphite structure, as shown in X-ray diffraction, to small and imperfect crystallites of graphite.

The Raman spectra of raw needle coke, N3 samples after 100 and 200 °C-heating are given in Fig. 4. In the Raman

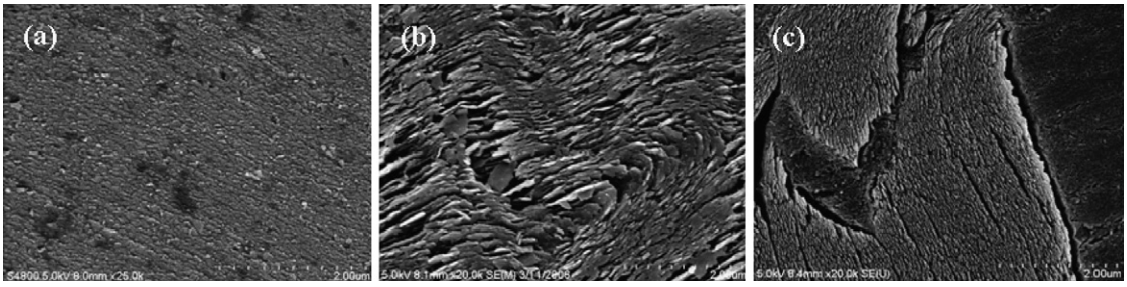

Fig. 2. Scanning electron micrographs of polished plane for (a) raw needle coke, (b) N3 after 100 °C-heating and (c) K1 after 100 °C-heating.

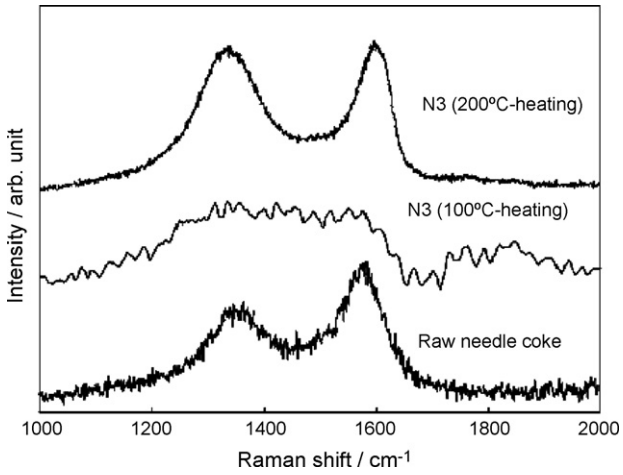

Fig. 4. Raman spectra of raw needle coke: N3 after 100 °C-heating, and N3 after 200 °C-heating.

spectrum of raw needle coke, two peaks at 1580 and 1360 cm^{-1} are observed, and the *R*-value, (i.e., the relative intensity proportion) of the 1360 to the 1580 cm^{-1} is 0.7. After oxidation treatment, however, no peak is observed in the range between 1200 and 1700 cm^{-1}. No detecting of spectrum peak may be caused by the destruction of inter-layer structure due to the formation of oxygen-containing groups. In the Raman spectrum of pyrolized needle coke, two peaks at 1580 and 1360 cm^{-1} appear again. However, the *R*-value of 1.0 in pyrolized needle coke is higher than that of raw needle coke. In general, the 1360 cm^{-1} line is observed at the SP^3 structure that lacks regularity, as in disordered graphite. Therefore, stronger detection of the 1360 cm^{-1} line at pyrolized needle coke indicates that there appear to be many structural defects in the graphene layer structure, as suggested by the assumption of the vigorous loss of the carbon atoms together with oxygen during the process of reduction.

3.2. Electrochemical performance of pyrolized and KOH-activated needle coke

The electrochemical performance of needle coke (N3) and KOH-activated needle coke (K1) as the electrode for an EDLC were examined. Fig. 5 shows (a) the first and (b) the second charge–discharge curves for cell capacitors using needle cokes of N3 after 200 °C-heating and K1 after 200 °C-heating. With the KOH-activated needle coke, the K1-cell was charged up to 3.5 V at first charge to induce a large capacitance. The data show that after a linear increase of capacitance in proportion to the voltage in the first charge, a gradual increase that deviates from the linear line is observed. However, after the second charge, the cell capacitor behaves linearly against the voltage, regardless of the number of charges–discharges. This behaviour, as reported previously [5], is associated with the electric field activation at the first charge, and after the second charge the capacitance is obtained in the pores formed between internal layers by the first charge. That is, the pyrolized needle coke produces a negligibly small electric double-layer when it is first dipped into an electrolyte solution. During the first charging process, however, the

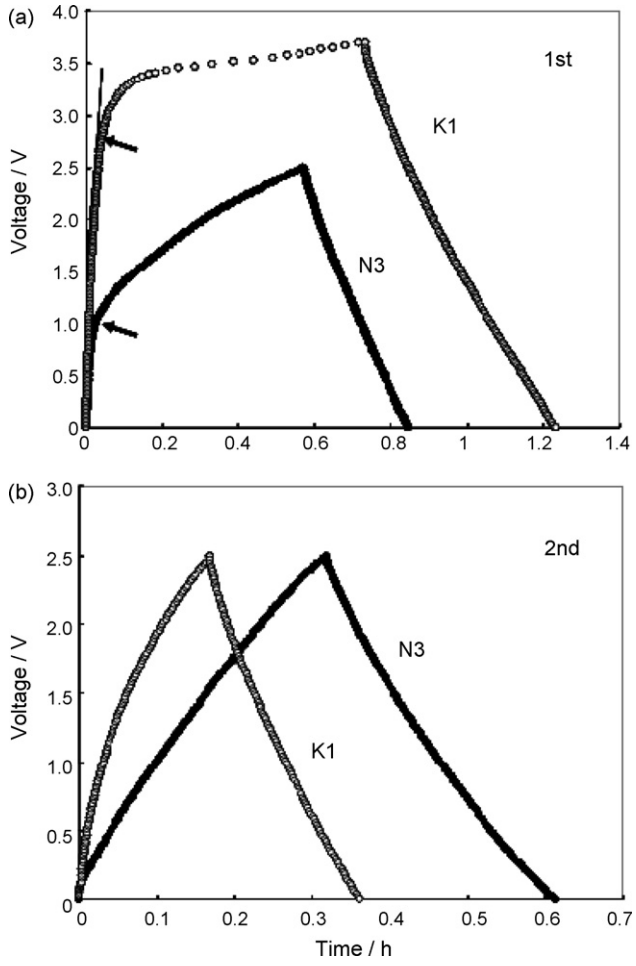

Fig. 5. (a) First and (b) second charge–discharge curves for capacitors using N3 after 200 °C-heating and K1 after 200 °C-heating.

intercalation of ions builds double-layers between the internal layers, and during the discharging process, the electrolyte ions go out. After that, the electrodes behave like conventional activated porous carbons with a high capacitance. During the first charge, the onset point, represented by an arrow in the figure, can be regulated as an intercalation starting voltage (ISV), and the ISVs of N3 and K1 indicate about 1.0 and 2.8 V respectively. In case of KOH activation, as it can be estimated that the inter-layer structure of needle coke is virtually unaffected by the activation process, the intercalation of electrolyte ions into the inter-layer of needle coke appears to occur at a high voltage. However, for the lower ISV of the N3-cell it is considered that the electrolyte ions can intercalate easily into the distorted graphene layer structure derived from the process of inter-layer expansion and shrinkage. The structural defects in the distorted graphene layer structure may introduce many small pores in the pyrolized needle coke during the first charge, resulting in a large capacitance.

The oxidation conditions and the specific capacitance of the pyrolized needle coke are summarized in Table 2. The specific capacitance per weight of the pyrolized needle coke and the electrode volume in the two-electrode system increase with increase in the ratio of $NaClO_3$/needle coke, and the maximum values in the N3 sample are 30.3 F g^{-1} and 26.9 F ml^{-1},

Table 2
Electrochemical properties of pyrolized needle cokes (N1–N4) after 200 °C-heating and K1 after 200 °C-heating

Sample	Electrode density (g ml^{-1})	Capacitance	
		F g^{-1}	F ml^{-1}
N1-cell	1.14	20.5	18.7
N2-cell	1.11	25.9	22.9
N3-cell	1.11	30.3	26.9
N4-cell	0.87	30.4	21.2
K1-cell	1.19	18.8	18.0

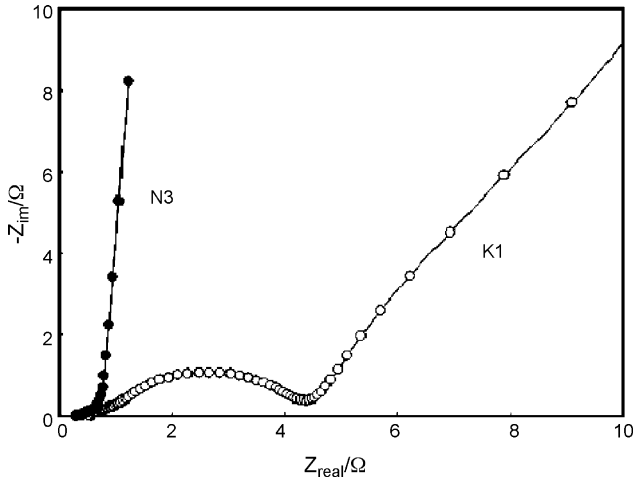

Fig. 6. AC impedance spectra for capacitors using N3 after 200 °C-heating and K1 after 200 °C-heating.

respectively. For the N4 sample, the specific capacitance per volume has a lower value than that of the N3 sample due to the lower density of the electrode.

The spectra (i.e., Nyquist plot) of the N3-cell and the K1-cell after the second charge–discharge are presented in Fig. 6.The spectra display a small semicircle at high frequency followed by a transition to linearity at low frequency. The ac spectrum of the N3-cell displays a vertical line close to 90° at low frequency, which indicates purely capacitive behaviour. On the other hand, the AC spectrum of the K1-cell has a line close to 45° in the low-frequency range. This is typical of a Warburg impedance. The internal resistance at 1 kHz for the N3-cell and the K1-cell is estimated to be 0.57 and 1.93 Ω, respectively. Therefore, it can be concluded that the structural features of the pyrolized needle coke allow the electrolyte to enter easily into the pores formed in the graphene layers, and this results in a low internal resistance.

4. Conclusions

The oxidation of needle cokes with a dilute nitric acid and sodium chlorate, combined with heat treatment, has been attempted to achieve an electrochemically active material with a large capacitance. As a comparison, KOH-activation of the same coke has been carried out. With increase in the amount of $NaClO_3$ added to the acidic solution, the oxygen content in needle coke is increased. The structure of needle cokes changes to the single phase of graphite oxide after oxidation treatment of the needle coke with acidic solution having an $NaClO_3$/needle coke composition ratio above 7.5. According to SEM observations, the oxidation treatment tends to induce an expanded graphene layer of needle coke, whereas the graphene layer of KOH-activated needle coke is almost unaffected. The calculated inter-layer distance of oxidized needle coke is 6.9 Å. However, after heating at 200 °C, the oxidized needle cokes are decomposed and reduce to a graphite structure with an inter-layer distance of 3.6 Å. From Raman spectrum, it is concluded that the pyrolized needle cokes have many defects in the inter-layer.

The first charge profile of a cell capacitor using pyrolized needle coke from graphite oxide shows that the charge takes place rapidly below 1.0 V and then very gradually increases up to 2.5 V. After the second charge–discharge, however, the capacitor behaves linearly, like a conventional capacitor. This electrochemical behaviour is related to electric field activation. A capacitor using pyrolized needle coke has a lower internal resistance of 0.57 Ω in 1 kHz, and a larger capacitance per weight and volume of 30.3 F g^{-1} and 26.9 F ml^{-1} in the two-electrode system over the potential range of 0–2.5 V, compared with a capacitor using KOH-activation of needle coke. This improved electrochemical performance is associated with a distorted graphene layer structure derived from the process of inter-layer expansion and shrinkage.

References

[1] M.F. Rose, C. Johnson, T. Owen, B. Stephen, J. Power Sources 47 (1994) 303–312.
[2] B.E. Conway, Electrochemical Supercapacitors, Kluwer Academic Publishers, New York, 1999, p. 12.
[3] J.R. Miller, Proceedings of the 12th International Seminar on Battery Technology and Applications, Deerfield Beach, FL, 1995.
[4] S. Nomoto, H. Nakata, K. Yoshioka, A. Yoshida, H. Yoneda, J. Power Sources 97 (2001) 807–811.
[5] M. Takeuchi, T. Maruyama, K. Koike, A. Kogami, T. Oyama, H. Kobayashi, Electrochemistry 69 (2001) 487–492.
[6] S. Mitani, S.I. Lee, S.H. Yoon, Y. Korai, I. Mochida, J. Power Sources 133 (2004) 298–301.
[7] S. Mitani, S.I. Lee, K. Saito, S.H. Yoon, Y. Korai, I. Mochida, Carbon 43 (2005) 2960–2968.
[8] W.S. Hummers Jr., R.E. Offeman, J. Am. Chem. Soc. 80 (1958) 1339.
[9] T. Nakajima, A. Maruchi, R. Hagiwara, Carbon 26 (1988) 357–361.